

# Scaling Properties of light (anti)nuclei and (anti)hypertriton production in Au+Au collisions at $\sqrt{s_{NN}} = 200$ GeV

Chen Gang\*, Chen Huan, Wang Jiang-Ling and Chen Zheng-Yu

*School of Mathematics and Physics, China University of Geosciences, Wuhan 430074,  
China.*

---

## Abstract

We present the scaling properties of mass number of light (anti)nuclei production in midrapidity Au + Au collisions at  $\sqrt{s_{NN}} = 200$  GeV based on the PACIAE + DCPC model. It is found that the integrated yield of light (anti)nuclei decreased exponentially with the increase of mass numbers which depends on the centrality, this properties of the system can be described quantitatively by temperature  $T$  at hadronic freeze-out, and the model results are consistent with STAR data. Furthermore, we found that the integrated yield of heavier (anti)nuclei per participant nucleon increases from peripheral to central collisions more rapidly than that of  $d(\bar{d})$ , indicating that the mass scale of light (anti)nuclei production was presented in relativistic heavy ion collisions. .

*Keywords:* Relativistic heavy ion collision, Antinuclei and Hypertriton, PACIA and DCPC Model, Scaling Properties

---

## 1. Introduction

The hot and dense matter formed in relativistic heavy ion collision experiments, which is similar to the fireball environment in the initial stages of the big bang, provides a good opportunity for studying the production of light (anti)nuclei.<sup>[1,2]</sup> The STAR Collaboration has reported their measurements of  ${}^3_{\Lambda}H$ ,  $\bar{{}^3_{\Lambda}H}$  and  $\bar{{}^4He}$  in Au+Au collisions at the top energy available at the BNL Relativistic Heavy Ion Collider (RHIC)<sup>[3,4]</sup>. The ALICE Collaboration has also published its preliminary  $\bar{d}$  yield of  $\sim 6 \times 10^{-5}$  measured in the proton-proton collisions at  $\sqrt{s} = 7$  TeV<sup>[5,6]</sup>.

In theory, light (anti)nuclei can be produced via two mechanisms. The first mechanism is direct production of nucleus-antinucleus pairs in elementary nucleon-nucleon or parton-parton interactions. However, because of their small

---

\*corresponding author

*Email address:* chengang1@cug.edu.cn (Chen Gang)

binding energies, such (anti)nuclei are likely to be dissociated in the medium before escaping. The second, and presumably dominant, mechanism for antinucleus production is via final-state coalescence<sup>[7,8,9]</sup>. The light (anti)nuclei and (anti)hypernuclei are usually studied by the transport models + the phase space coalescence model<sup>[10,11,12]</sup> and/or the statistical model<sup>[13,14,15,16]</sup> etc. For example, their production rate can be described by both thermodynamic model and coalescence model. In thermodynamic model, the system created is characterized by the chemical freeze-out temperature ( $T_{ch}$ ), kinetic freeze-out temperature ( $T_{kin}$ ), as well as the baryon and strangeness chemical potential  $\mu_B$  and  $\mu_S$ . An (anti)nucleus is regarded as an object with energy  $E_A = Am_p$  ( $A$  is the atomic mass number,  $m_p$  is the mass of proton) emitted by the fireball<sup>[14]</sup>. The production rates are proportional to the Boltzmann factor  $e^{-m_p A/T}$ <sup>[4]</sup>. In a microscopic picture, a light (anti)nucleus is produced during the last stage of the collision process via the strong correlation between the constituent nucleons in their phase space<sup>[17,18,19,20]</sup>.

Recently, we have proposed an approach the dynamically constrained phase-space coalescence model (DCPC)<sup>[21]</sup> which is based on the final hadronic state generated by a parton and hadron cascade model PACIAE<sup>[22]</sup>. Using this method, the light nuclei (anti-nuclei) yields, transverse momentum distribution, and the rapidity distribution in non-single diffractive proton-proton collisions at  $\sqrt{s} = 7$  TeV<sup>[21]</sup> are predicted, and the light nuclei (anti-nuclei) and hypernuclei (anti-hypernuclei) productions<sup>[23]</sup> and its centrality dependence<sup>[24]</sup> in the Au+Au collisions at  $\sqrt{s_{NN}} = 200$  GeV are investigated.

Previous studies have shown that light nuclei production depends on the mass number  $A$  in Ultrarelativistic Heavy-Ion Collisions<sup>[25]</sup>, and yields of light (anti)nuclei and (anti)hypertriton per participant nucleon (Npart) depends on the mass number in Au+Au collisions at  $\sqrt{s_{NN}} = 200$  GeV<sup>[23]</sup>. In this paper, we study the yields of light (anti)nuclei and (anti)hypertriton depending on the mass number in Au+Au collisions at  $\sqrt{s_{NN}} = 200$  GeV with the PACIAE + DCPC model in an attempt to shed light upon the possible production mechanisms.

## 2. Models

The parton and hadron cascade model PACIAE<sup>[22]</sup> is based on PYTHIA 6.4<sup>[26]</sup> and is devised mainly for the nucleus-nucleus collisions. In the PACIAE model, firstly, the nucleus-nucleus collision is decomposed into the nucleon-nucleon ( $NN$ ) collisions according to the collision geometry and  $NN$  total cross section. Each  $NN$  collision is described by the PYTHIA model with the string fragmentation switching off and the diquarks (antidiquarks) randomly breaking into quarks (anti-quarks). So the consequence of a  $NN$  collision is a partonic initial state composed of quarks, anti-quarks, and gluons. Provided all  $NN$  collisions are exhausted, one obtains a partonic initial state for a nucleus-nucleus collision. This partonic initial state is regarded as the quark-gluon matter (QGM) formed in relativistic nucleus-nucleus collisions. Second, the parton rescattering proceeds. The rescattering among partons in QGM is randomly considered by the  $2 \rightarrow 2$  LO-pQCD parton-parton cross sections<sup>[27]</sup>. In addition, a  $K$  factor is

introduced here to account for higher order and non-perturbative corrections. Third, hadronization happens after parton rescattering. The partonic matter can be hadronized by the Lund string fragmentation regime<sup>[26]</sup> and/or the phenomenological coalescence model<sup>[22]</sup>. Finally, the hadronic matter continues rescattering until the hadronic freeze-out (the exhaustion of the hadron-hadron collision pairs). We refer to<sup>[22]</sup> for the details.

In quantum statistical mechanics<sup>[28]</sup> one can not precisely define both position  $\vec{q} \equiv (x, y, z)$  and momentum  $\vec{p} \equiv (p_x, p_y, p_z)$  of a particle in the six-dimension phase space, because of the uncertainty principle  $\Delta\vec{q}\Delta\vec{p} \geq h^3$ . We can only say that this particle lies somewhere within a six-dimension quantum box or state with a volume of  $\Delta\vec{q}\Delta\vec{p}$ . A particle state occupies a volume of  $h^3$  in the six-dimension phase space<sup>[28]</sup>. Therefore one can estimate the yield of a single particle by defining an integral  $Y_1 = \int_{H \leq E} \frac{d\vec{q}d\vec{p}}{h^3}$ , where  $H$  and  $E$  are the Hamiltonian and energy of the particle, respectively. Similarly, the yield of  $N$  particle cluster can be estimated as following integral<sup>[21,23]</sup>

$$Y_N = \int \dots \int_{H \leq E} \frac{d\vec{q}_1 d\vec{p}_1 \dots d\vec{q}_N d\vec{p}_N}{h^{3N}}. \quad (1)$$

In addition, the Eq. (1) must satisfy the constraint condition following

$$m_0 \leq m_{inv} \leq m_0 + \Delta m, \quad (2)$$

$$q_{ij} \leq D_0, \quad (i \neq j; i, j = 1, 2, \dots, N). \quad (3)$$

Where,

$$m_{inv} = \left[ \left( \sum_{i=1}^N E_i \right)^2 - \left( \sum_{i=1}^N \vec{p}_i \right)^2 \right]^{1/2}, \quad (4)$$

and  $E_i, \vec{p}_i (i = 1, 2, \dots, N)$  are the energies and momenta of particles, respectively.  $m_0$  and  $D_0$  stands for, respectively, the rest mass and diameter of light (anti)nuclei,  $\Delta m$  refers to the allowed mass uncertainty, and  $q_{ij} = |\vec{q}_i - \vec{q}_j|$  is the vector distance between particle  $i$  and  $j$ . Because the hadron position and momentum distributions from transport model simulations are discrete, the integral over continuous distributions in Eq. (1) should be replaced by the sum over discrete distributions<sup>[24]</sup>.

### 3. The mass number dependence of light (anti)nuclei production at RHIC

First we produce the final state particles using the PACIAE model. In the PACIAE simulations we assume that hyperons are heavier than  $\Lambda$  decayed already. The model parameters are fixed on the default values given in PYTHIA<sup>[26]</sup>. However, the  $K$  factor as well as the parameters  $\text{parj}(1)$ ,  $\text{parj}(2)$ , and  $\text{parj}(3)$ , relevant to the strange production in PYTHIA<sup>[26]</sup>, are given by fitting the STAR data of  $\Lambda$ ,  $\bar{\Lambda}$ ,  $\Xi^-$ , and  $\bar{\Xi}^-$  in Au+Au collisions at  $\sqrt{s_{NN}} = 200$  GeV<sup>[29]</sup>. The fitted

parameters of  $K=3$  (default value is 1 or 1.5<sup>[26]</sup>),  $\text{parj}(1) = 0.12$  (0.1),  $\text{parj}(2) = 0.55$  (0.3), and  $\text{parj}(3) = 0.65$  (0.4) are used to generate  $1.02 \times 10^8$  minimum-bias events by the PACIAE model for Au+Au collisions at  $\sqrt{s_{\text{NN}}} = 200$  GeV with  $|y| < 1$  and  $0 < p_t < 5$  acceptances<sup>[23]</sup>.

Then, the yields  $dN/dy$  of  $d$  ( $\bar{d}$ ),  ${}^3\text{He}$  ( ${}^3\overline{\text{He}}$ ),  ${}^3_{\Lambda}\text{H}$  ( ${}^3_{\Lambda}\overline{\text{H}}$ ), as well as  ${}^4\text{He}$  ( ${}^4\overline{\text{He}}$ ) are calculated by the DCPC model for different centrality bins of 0-5%, 5-10%, 10-15%, 15-20%, 20-30%, 30-40%, and 40-60%, as shown in Tab. 1. We can see from Tab. 1 that the yields  $dN/dy$  of light (anti)nuclei and (anti)hypertritons decrease (or increase) with the increase of centrality (or  $N_{\text{part}}$ ); the yields of antinuclei are less than those of their corresponding nuclei; and the greater the mass is, the lower the yield is.

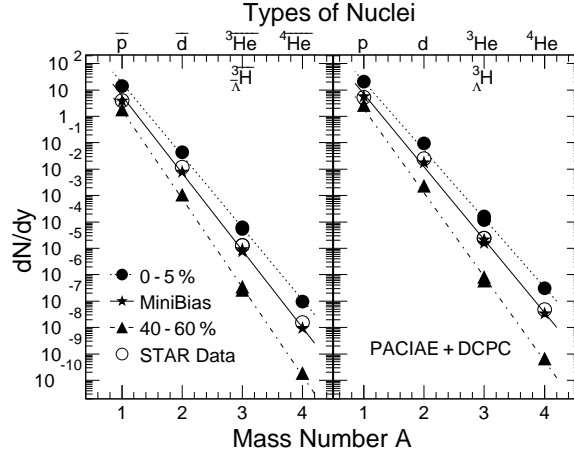


Figure 1: Atomic number dependence of the integrated yield  $dN/dy$  of light (anti)nuclei ( $d, \bar{d}$ ,  ${}^3_{\Lambda}\text{H}, {}^3_{\Lambda}\overline{\text{H}}$ ,  ${}^3\text{He}, {}^3\overline{\text{He}}$ ,  ${}^4\text{He}, {}^4\overline{\text{He}}$ ) in different centrality bins of 0-5%, 40-60%, and MiniBias, respectively. The solid symbols are calculated by PACIAE+DCPC model in the midrapidity Au+Au collisions at the RHIC energy, while the open ones represent the data points extracted by the STAR experiment<sup>[17,4]</sup>. The lines represent the Model result's fit for the positive matters (right) and antimatters (left) with formula  $e^{-Am_p/T}$ .

In order to further explore the mass and/or centrality dependence of light (anti)nuclei production, we study the integrated yield  $dN/dy$  of light (anti)nuclei as a function of atomic mass number  $A$  and/or centrality. Fig. 1 shows the distributions of integrated yield  $dN/dy$  of light (anti)nuclei ( $d, \bar{d}$ ,  ${}^3_{\Lambda}\text{H}, {}^3_{\Lambda}\overline{\text{H}}$ ,  ${}^3\text{He}, {}^3\overline{\text{He}}$ ,  ${}^4\text{He}, {}^4\overline{\text{He}}$ ) vs atomic mass number  $A$  with  $A = 1$  to  $A = 4$  in different centrality bins of 0-5%, 40-60%, and MiniBias, respectively. The solid symbols are calculated by PACIAE+DCPC model in the midrapidity Au+Au collisions at the RHIC energy, while the open ones represent the data points extracted from the STAR experiment<sup>[17,4]</sup>. Obviously, the model results are consistent with STAR data<sup>[17,4]</sup>, indicating that the selection parameter  $\Delta m$  calculated yields of light (anti)nuclei in Tab. 1 are appropriate.

Table 1: Integrated yields  $dN/dy$  calculated by PACIAE+DCPC model of  $\bar{d}$ ,  $d$ ,  $\frac{3}{\Lambda}H$ ,  $\frac{3}{\Lambda}H$ ,  $\frac{3}{\Lambda}He$ ,  $\frac{3}{\Lambda}He$ ,  $\frac{4}{\Lambda}He$  and  $\frac{4}{\Lambda}He$  in midrapidity Au+Au collisions of  $\sqrt{s_{NN}} = 200$  GeV.  $\langle N_{part} \rangle$  is shown for each centrality.

Centrality	0 – 5%	5 – 10%	10 – 15%	15 – 20%	20 – 30%	30 – 40%	40 – 60%
$\langle N_{part} \rangle$	334	295	252	213	164	108	54
$d^a$	0.0964	0.0837	0.0537	0.0389	0.0224	0.00936	0.00239
$\bar{d}^a$	0.0433	0.0383	0.0244	0.0179	0.0101	0.00425	0.00107
${}^3He^b$	1.60E-04	1.17E-04	6.52E-05	3.76E-05	1.60E-05	3.78E-06	8.19E-07
$\frac{3}{\Lambda}He^b$	6.52E-05	4.88E-05	3.05E-05	1.69E-05	7.23E-06	1.71E-06	3.53E-07
$\frac{3}{\Lambda}H^b$	1.21E-04	9.11E-05	4.95E-05	2.97E-05	1.28E-05	2.90E-06	6.07E-07
$\frac{3}{\Lambda}H^b$	5.59E-05	4.33E-05	2.43E-05	1.43E-05	6.33E-06	1.39E-06	2.71E-07
$\frac{4}{\Lambda}He^c$	5.14E-07	3.22E-07	1.44E-07	9.36E-08	2.27E-08	3.90E-09	1.13E-09
$\frac{4}{\Lambda}He^c$	1.70E-07	7.45E-08	4.22E-08	2.46E-08	7.59E-09	1.16E-09	3.32E-10

<sup>a</sup> calculated with  $\Delta m = 0.00035$  GeV for  $d, \bar{d}$ .

<sup>b</sup> calculated with  $\Delta m = 0.00055$  GeV for  ${}^3He, \frac{3}{\Lambda}He, \frac{3}{\Lambda}H, \frac{3}{\Lambda}H$ .

<sup>c</sup> calculated with  $\Delta m = 0.0007$  GeV for  $\frac{4}{\Lambda}He, \frac{4}{\Lambda}He$ .

One can see from Fig. 1, that the yields of light (anti)nuclei and (anti)hypertriton all decrease rapidly with the increase of atomic mass number  $A$ , and the integrated yield  $dN/dy$  span almost 5 orders of magnitude with striking exponential behavior. In this figure the curve is fitted to the data point using equation as<sup>[25,31,32]</sup>

$$E_A \frac{d^3 N_A}{d^3 P_A} \propto E_A e^{-m_p A/T}, \quad (5)$$

where  $E_A \frac{d^3 N_A}{d^3 P_A}$  stands for the invariant yield of (anti)nuclei,  $P_A$  is the momentum of (anti)nuclei, and  $T$  is the temperature at hadronic freeze-out. The temperature parameters  $T$ , fitting to the integrated yield  $dN/dy$  of antinuclei in Fig. 1 by Eq.(5), are  $(149 \pm 3)$  MeV for centrality of 0-5%,  $(142 \pm 4)$  MeV for MiniBias events, and  $(125 \pm 6)$  MeV for centrality of 40-60%, respectively. The value of the temperature  $T$  for light nuclei are close to those of antinuclei within the error range. Obviously, since the temperature of peripheral collision is lower than central collisions, so their yield decrease faster with increasing of mass number  $A$ .

For a further analysis on the effects of centrality, we show, in Fig.2, the yields  $dN/dy$  of  $d, \bar{d}, \frac{3}{\Lambda}H, \frac{3}{\Lambda}H, {}^3He, \frac{3}{\Lambda}He, {}^4He$ , and  $\frac{4}{\Lambda}He$  as functions of centrality in Au+Au collisions at  $\sqrt{s_{NN}} = 200$  GeV. All data points are normalized to the values in the central collisions (0-5%). The centrality dependence of the antiproton and antilambda yield is also shown for comparison<sup>[33]</sup>. It shows that the yields of light (anti)nuclei and (anti)hypertriton decrease with the increase of the centrality. Furthermore, this distribution properties of light (anti)nuclei and (anti)hypertriton production mainly depend on their mass number, i.e. the greater the mass number is, the faster the yield decreases.

The integrated yield is dominated by the low  $p_t$  region, where particle production is driven mainly by soft processes. The yield per participant nucleon may reflect the formation probability of a hadron from the bulk. We would then expect it to be sensitive to the density of the light nuclei's constituent hadrons in the system. We define a relative yield  $R_{CY}(N_{\text{part}})$  as a measure of the (anti)nuclei production's dependence on the collision system's size and density:

$$R_{CY}(N_{\text{part}}) = \frac{(dN/dy)/N_{\text{part}}}{[(dN/dy)/N_{\text{part}}]_{\text{Peripheral}}}. \quad (6)$$

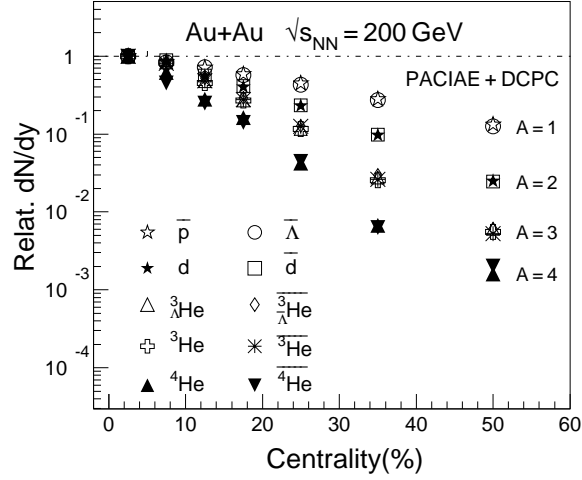


Figure 2: The integrated yield  $dN/dy$  of  $\bar{p}$ ,  $\bar{\Lambda}$ ,  $d$ ,  $\bar{d}$ ,  ${}^3_{\Lambda}\bar{H}$ ,  $\overline{{}^3_{\Lambda}H}$ ,  ${}^3He$ ,  $\overline{{}^3He}$ ,  ${}^4He$ ,  $\overline{{}^4He}$  in the midrapidity Au+Au collisions at  $\sqrt{s_{NN}} = 200$  GeV, normalized to the central collisions (0-5%), as a function of centrality.

In Fig. 3(A) we show the relative yield  $R_{CY}(N_{\text{part}})$  of  $d$ ,  $\bar{d}$ ,  ${}^3_{\Lambda}H$ ,  $\overline{{}^3_{\Lambda}H}$ ,  ${}^3He$ ,  $\overline{{}^3He}$ ,  ${}^4He$ , and  $\overline{{}^4He}$ , as functions of  $N_{\text{part}}$ . All data points are normalized to the values obtained in the peripheral collisions (40-60%)<sup>[33]</sup>. It shows that the yields of light (anti)nuclei and (anti)hypertriton per participant nucleon increase rapidly with the increase of the number of participant  $N_{\text{part}}$  as the  $N_{\text{part}} > 100$ . Obviously, this distribution properties of light (anti)nuclei and (anti)hypertriton production in Au+Au collisions at  $\sqrt{s_{NN}} = 200$  GeV depend on their mass number, i.e. the greater the mass number, the faster the increase is in yield. For a more quantitative comparison, we define a relative yield invariants  $R_{CYA}(N_{\text{part}})$  as

$$R_{CYA}(N_{\text{part}}) = {}^A\sqrt{R_{CY}(N_{\text{part}})}, \quad (7)$$

where  $A$  is the atomic mass number. We show the results of  $R_{CYA}(N_{\text{part}})$ , with data points normalized to the values in the peripheral collisions (30-40%), in

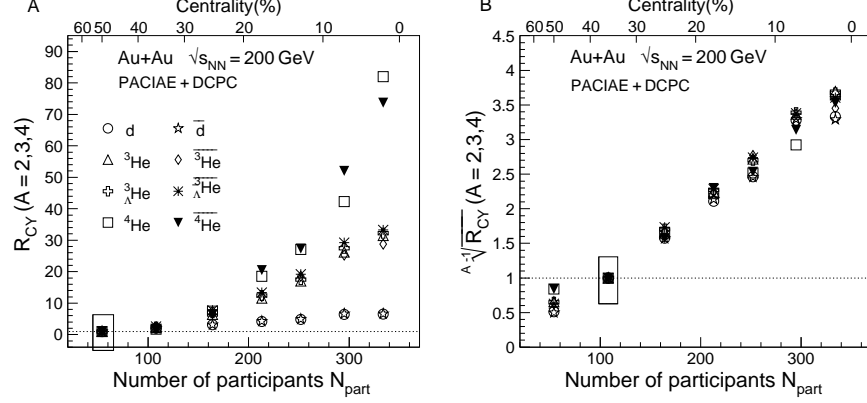


Figure 3: (A) The integrated yield  $dN/dy$  at midrapidity for  $d, \bar{d}, {}^3_\Lambda\text{H}, \bar{{}^3_\Lambda\text{H}}, {}^3\text{He}, \bar{{}^3\text{He}}, {}^4\text{He}, \bar{{}^4\text{He}}$  divided by  $N_{part}$ , normalized to the peripheral collisions (40-60%), plotted as a function of  $N_{part}$ . (B) Relative yield invariants  $A^{-1} \sqrt{R_{CY}}$  as a function of  $N_{part}$  (cf. text for details). The results are calculated by PACIAE+DCPC model in Au+Au collisions at  $\sqrt{s_{NN}} = 200$  GeV.

Fig.3(B). We were surprised to find that the datum for all different (anti)nuclei and (anti)hypertriton locate on the same straight line, i.e. the distribution of the relative yield invariants  $R_{CYA}(N_{part})$  is independent on the number or type of the constituent hadrons. Herein, we found a scaling property of (anti)nuclei and (anti)hypernuclei production in relativistic heavy ion collisions. We expect this scaling property would provide us a new clue to explore the hadronic final state, as well as the (anti)nuclei and (anti)hypernuclei production mechanism in relativistic heavy ion collisions.

#### 4. Conclusion

In this paper we use the PACIAE+DCPC model to investigate the mass number dependence of light (anti)nuclei and (anti)hypertriton production in Au+Au collisions at top RHIC energy. The results show that the yields of light (anti)nuclei decrease rapidly with the increase of atomic mass number, and the integrated yield  $dN/dy$  span almost 5 orders of magnitude with striking exponential behavior which depends on the centrality. This properties of the system can be described quantitatively by temperature  $T$  at hadronic freeze-out, and the model results are consistent with STAR data. In addition, we studied the relative yields per  $N_{part}$  of light (anti)nuclei, normalized to the values obtained in the peripheral collisions. It is found that the yields of light antinuclei and antihypertriton production per participant nucleon increase linearly with  $N_{part}$  as  $N_{part} > 100$ , and the yield of heavy nuclei increases more rapidly than that of light nuclei. We found that the light (anti)nuclei and (anti)hypertriton production in Au+Au collisions at  $\sqrt{s_{NN}} = 200$  GeV exist an mass number scaling

property. We expect that this scaling characteristics can be tested in heavy ion collision experiments.

#### ACKNOWLEDGMENT

Finally, we acknowledge the financial support from NSFC (11305144, 11303023) and Central Universities (GUGL 100237,120829,130249,130605) in China. The authors thank Nu Xu and Ben-Hao Sa for helpful discussions.

#### References

- [1] S. S. Adler et al.(PHENIX Collaboration), Phys. Rev. Lett.,**94**, 122302 (2005).
- [2] B.I. Abelev et al.(STAR Collaboration), Phys. Lett. B **655**, 104 (2007).
- [3] B. I. Abelev et al. (STAR Collaboration), Science **328**, 58 (2010).
- [4] H. Agakishiev et al.(STAR Collaboration), Nature **473**, 353 (2011);
- [5] N. Sharma(ALICE Collaboration), Acta Physica Polonica B **5(2)** 605(2012).
- [6] N. Sharma(ALICE Collaboration), J. Phys. G: Nucl. Part. Phys. **38**, 124189 (2011).
- [7] S. T. Butler and C. A. Pearson, Phys. Rev. **129**, 836 (1963).
- [8] A.Schwarzschild and C. Zupancic, Phys. Rev. **129**, 854 (1963).
- [9] H. H. Gutbrod et al., Phys. Rev. Lett. **37** 667 (1976).
- [10] R. Mattiello, H. Sorge, H. Stöcker, and W. Greiner, Phys. Rev. C **55**, 1443 (1997).
- [11] L. W. Chen and C. M. Ko, Phys. Rev. C **73**, 044903 (2006).
- [12] S. Zhang, J. H. Chen, H. Crawford, D. Keane, Y. G. Ma, and Z. B. Xu, Phys. Lett. B **684**, 224 (2010).
- [13] V. Topor Pop and S. Das Gupta, Phys. Rev. C **81**, 054911 (2010).
- [14] A. Andronic, P. Braun-Munzinger, J. Stachel, and H. Stöcker, Phys.Lett. B **697**, 203 (2011).
- [15] L. Xue, Y. G. Ma, J. H. Chen and S. Zhang, Phys. Rev. C **85**, 064912 (2012).
- [16] J. Steinheimer, K. Gudima, A. Botvina, I. Mishustin, M. Bleicher, and H. Stoecker, Phys. Lett. **B714**, 85(2012).
- [17] B. I. Abelev et al. (The STAR Collaboration), arXiv:0909.0566 [nucl-ex].



- [18] H. Sato, K. Yazaki, et al., Phys. Lett. B **98**, 153 (1981).
- [19] R. Scheibl and U. Heinz, Phys. Rev. C **59**, 1585 (1999).
- [20] S. Albergo, R. Bellwied, M. Bennett, et al. Phys. Rev. C **65**, 034907 (2002).
- [21] Y. L. Yan, G. Chen, X. M. Li, et al. Phys. Rev. **C85**, 024907(2012).
- [22] B. H. Sa, D. M. Zhou, Y. L. Ya, et al. Comput. Phys. Commun. **183**, 333 (2012).
- [23] G. Chen, Y. L. Yan, D. S. Li, et al. Phys. Rev. **C86**, 054910(2012).
- [24] G. Chen, H. Chen, J. Wu, et al. Phys. Rev. **C88**, 034908(2013).
- [25] T. A. Armstrong(E864 Collaboration),Phys. Rev. Lett. **83**, 26 (1999).
- [26] T. Sjöstrand, S. Mrenna, and P. Skands, J. High Energy Phys. **05**, 026 (2006).
- [27] B. L. Combridge, J. Kripfgang, and J. Ranft, Phys. Lett. **B70**, 234 (1977).
- [28] K. Stowe, A introduction to thermodynamics and statistical mechanics, Combridge, 2007; R. Kubo, Statistical Mechanics, North-Holland Publishing Company, Amsterdam, 1965.
- [29] J. Adams et al.(STAR Collaboration), Phys. Rev. Lett. **98** , 062301 (2007)
- [30] J.Cleymans, B.Kampfer, M.Kaneta,S.Wheaton, N.Xu, Phys. Rev. **C 71**, 054901 (2005).
- [31] P. Braun-Munzinger, J. Stachel, J.P. Wessels, N. Xu, Phys. Lett. **B 344**, 43 ( 1995).
- [32] H. van Hecke, H. Sorge, and N. Xu, Phys. Rev. Lett. **81**, 5764 (1998).
- [33] J. Adams et al. (STAR Collaboration), Phys. Rev. Lett. **92**, 112301 (2004).
- [34] W. Greiner. Int. J. Mod. Phys. E: NUCL. PHYS. **5**, 1(1996).
- [35] Y. G. Ma, J. H. Chen, L. Xue, Front. Phys.,**7(6)**, 637 (2012).